Andrew J. Woods, Ka Lun Yuen, and Kai S. Karvinen, "Characterizing crosstalk in anaglyphic stereoscopic images on LCD monitors and plasma displays" in Journal of the Society for Information Display, Volume 15, Issue 11, pp. 889-898, November 2007. www.AndrewWoods3D.com

Characterizing crosstalk in anaglyphic stereoscopic images on LCD monitors and plasma displays

Andrew J. Woods
Ka Lun Yuen
Kai S. Karvinen

Abstract — In 1853, William Rollman[1] developed the inexpensive and easy to use anaglyph method for displaying stereoscopic images. Although it can be used with nearly any type of full-color display, the anaglyph method compromises the accuracy of color reproduction, and it often suffers from crosstalk (or ghosting) between the left- and right-eye image channels. Crosstalk degrades the ability of the observer to fuse the stereoscopic image, and hence reduces the quality of the 3-D image. Crosstalk is present in various levels with most stereoscopic displays; however, it is often particularly evident with anaglyphic 3-D images. This paper summarizes the results of two projects that characterized the presence of anaglyphic crosstalk due to spectral issues on 13 LCD monitors, 14 plasma displays, and a CRT monitor when used with 25 different pairs of anaglyph 3-D glasses. A mathematical model was used to predict the amount of crosstalk in anaglyphic 3-D images when different combinations of displays and glasses are used, and therefore highlight displays, glasses, and combinations thereof which exhibit lower levels of crosstalk when displaying anaglyphic 3-D images.

Keywords — *Anaglyph, 3-D, stereoscopic, crosstalk, ghosting, LCD monitors, plasma displays, CRT displays.*

1 Introduction

The anaglyph method of displaying stereoscopic images uses a complementary color-coding technique to send separate left and right views to an observer's two eyes. The two perspective images of a stereo-pair are stored in complementary color channels of the display, and the observer wears a pair of glasses containing color filters which act to pass the correct image but block the incorrect image to each eye.

For example, if a red/cyan anaglyph is used, the left perspective image is stored in the red color channel and the right perspective image is stored in the blue and green color channels (blue + green = cyan), and the observer wears a pair of anaglyph 3-D glasses with the left-eye filter red and the right-eye filter cyan.

The main advantages of the anaglyph 3-D method are its simplicity, low cost, and compatibility with any full-color display. The main disadvantages are its inability to accurately depict full-color images, and commonly the presence of crosstalk. Crosstalk (or ghosting) is the leaking of an image to one eye when it is intended exclusively for the other eye. For example, the left eye should only be able to see the left perspective image, but due to crosstalk, the left eye may see a small proportion of the right perspective image. Crosstalk occurs with most stereoscopic displays and results in reduced image quality and difficulty of fusion if the amount of crosstalk is large.

This paper considers the two spectral contributors to anaglyphic crosstalk: display spectral response and anaglyph glasses spectral response. Two other possible contributors to anaglyph ghosting, image compression and image encoding/transmission,[2] are not explored in this paper.

Figure 1 provides an illustration of the process of crosstalk in anaglyph stereoscopic images due to spectral leakage (as illustrated for the red/cyan method). Firstly, the display has a specific spectral output for the red, green, and blue color channels. Usually the left perspective image is stored in the red color channel and the right perspective image is stored in the green and blue color channels (cyan). Second, the red/cyan anaglyph 3-D glasses used to view the anaglyph display also have a certain spectral transmission response for the left and right eye filters. Here the left filter predominantly transmits red light but with a little bit of transmission in the green band, and the right filter predominantly transmits blue and green light but with a little bit of transmission in the red band. Due to the non-ideal nature of the display and the glasses, some light from the right (cyan) color channel leaks through the left (red) eye filter. Similarly, some light from the left (red) color channel leaks. This is in addition to the transmission of the intended image through the left- and right-eye filters. Therefore, the left eye predominantly sees the left perspective image but with a small amount of the right perspective image visible, and the right eye predominantly sees the right perspective image but with a small amount of the left perspective image visible.

This paper carries on from the work of Woods and Rourke[2] which considered anaglyph ghosting with cathode-ray tube (CRT) monitors, one liquid-crystal display (LCD) monitor, and a mixture of LCD and digital light processing (DLP) projectors. This paper focuses on anaglyph ghosting on LCD monitors and plasma displays with 13 LCD moni-

The authors are with the Centre for Marine Science & Technology, Curtin University of Technology, GPO Box U1987, Perth, WA 6845 Australia; telephone +61-8-9266-7920, fax –4799, e-mail: A.Woods@cmst.curtin.edu.au.

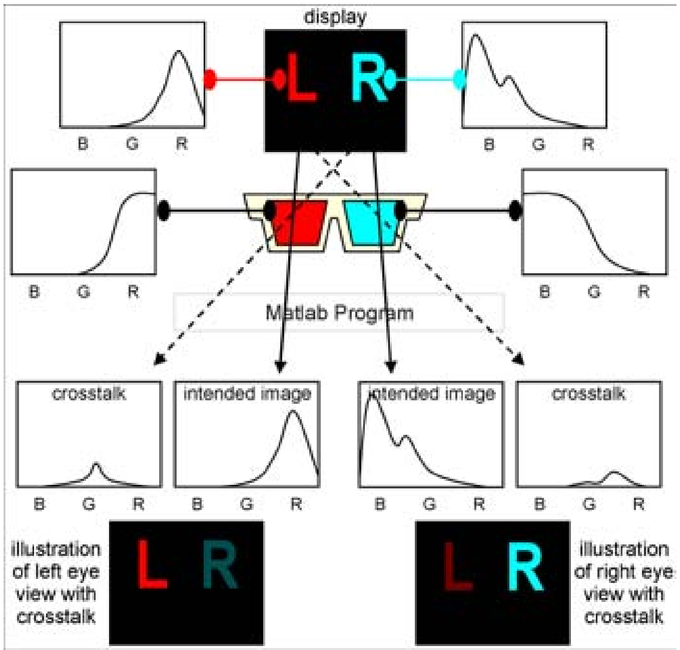

FIGURE 1 — Illustration of the process of anaglyph spectral ghosting and its simulation in this project. From the top: (1) Spectral response of display, (2) spectral response of anaglyph glasses, (3) simulation of ghosting using a computer program, (4) spectral output characteristic of crosstalk and intended image, and (5) visual illustration of left- and right-eye view with crosstalk.

tors and 14 plasma-displays panels (PDPs) tested. A CRT monitor was also tested for comparison purposes. All data for this project was measured using more accurate equipment than was available in the previous study.[2]

This paper only examines crosstalk in red/cyan anaglyph stereoscopic images, although the simulation methods discussed could also be applied to blue/yellow or green/magenta anaglyphs.

2 Experimental method

The first step was to measure the spectral output of the displays using a manually calibrated Ocean Optics USB2000 spectroradiometer. Table 1 itemizes the displays tested – consisting of 13 LCD computer monitors, 14 PDPs, and one CRT monitor.

Each display was connected to a PC which displayed a slide show consisting of a plain white slide (R = G = B = 255), a plain red slide (R = 255, G = B = 0), a plain green slide (R = B = 0, G = 255), a plain blue slide (R = G = 0, B = 255), and a plain black slide (R = G = B = 0). The spectroradiometer was used to measure the spectrum of each of these slides (as displayed on each display) and the data collected on a PC.

The second step was to measure the transmission spectrum of a large selection of anaglyph 3-D glasses using a PG Instruments T90+ UV/Vis spectrophotometer. A total of 50 pairs of anaglyph glasses were tested[3]; however, only 25 pairs are reported here for the sake of brevity.

TABLE 1 — Listing of the tested displays.

Tag	Display Make and Model
LCD01	Samsung SyncMaster 171s
LCD02	Benq FP731
LCD03	NEC MultiSync LCD 1760V
LCD04	Acer AL1712
LCD05	Acer FP563
LCD06	Benq FP71G
LCD07	Benq FP71G+S
LCD08	Philips 150S3
LCD09	Hewlett Packard HPL1706
LCD11	Samsung SyncMaster 740N
LCD12	Philips 190s
LCD13	Samsung SyncMaster 913B
LCD14	ViewSonic VX922
PDP01	LG DT-42PY10X
PDP02	Fujitsu P50XHA51AS
PDP03	NEC PX-50XR5W
PDP04	Panasonic TH-42PV60A
PDP05	Samsung PS-42C7S
PDP06	LG RT-42PX11
PDP07	NEC PX-42XM1G
PDP08	Sony PFM-42V1
PDP09	Sony FWD-50PX2
PDP10	Hitachi 55PD8800TA
PDP11	Hitachi 42PD960BTA
PDP12	Pioneer PDP-507XDA
PDP13	Pioneer PDP-50HXE10
PDP14	Fujitsu PDS4221W-H
CRT	Mitsubishi Diamond View VS10162

Note: Due to manufacturing variation or experimental error, the results provided in this paper should not be considered to be representative of all displays of that particular brand or model.

The third step was to use a specially developed Matlab computer program to calculate the presence of crosstalk in the anaglyph images for different display and glasses combinations. With reference to Fig. 1, the program first loads and resamples the display and filter spectral data so that all data is on a common x-axis coordinate system. Next, the program determines the display's cyan spectral output by adding the green and blue color channel data of the display. The program then multiplies the red display spectrum with the red filter's spectral response to obtain the intended image curve for the red eye, multiplies the cyan display spectrum with the cyan filter's spectrum to obtain the intended image curve for the cyan eye, multiplies the red display spectrum with the cyan filter's spectral response to obtain the crosstalk curve for the cyan eye, and multiplies the cyan display spectrum with the red filter's spectrum to obtain the crosstalk curve for the red eye.

The program also scales these result curves to include the human-eye response to light by multiplying by the curve shown in Fig. 2, which shows the CIE (International Commission on Illumination) model for simulating photopic (bright light) human-eye sensitivity to light.[4]

The crosstalk percentage for each eye is then calculated by dividing the area under the crosstalk curve by the area under the intended signal curve for each eye and multiplying by 100. The overall crosstalk factor for a particular

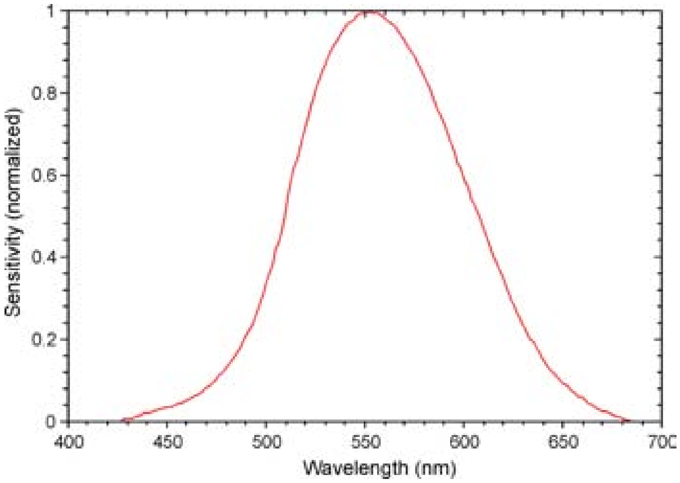

FIGURE 2 — CIE 1931 standard normalized photopic human-eye response.

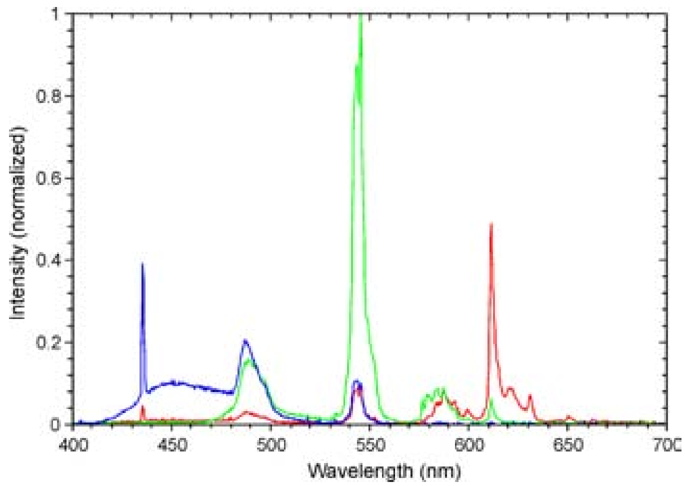

FIGURE 3 — Color spectrum of an example LCD monitor (LCD04).

pair of glasses in combination with a particular display is the sum of the left- and right-eye percentage crosstalk values. It should be noted that the overall crosstalk factor is not a percentage, but rather a number that allows the comparison of different glasses/display combinations. The program also automates the process of performing a cross comparison of all the displays against all of the glasses.

3 Results

3.1 Display device results

The spectral output measurement of 13 different LCD monitors, 14 different PDP monitors, and one CRT monitor are reported in this study.

Figure 3 shows the spectral output of an example LCD monitor (LCD04). All of the LCD monitors tested used cold cathode fluorescent lamp (CCFL) backlights. CCFLs are a form of mercury-vapor fluorescent lamp that generate visible light by energizing the gas in the fluorescent tube so that it emits ultraviolet rays which in turn causes the phosphor material that coats the inside surface of the tube to emit visible light. The spectrum of a CCFL is fairly broad but with many notable narrow peaks. Although the spectral output of the raw CCFL was not measured in any of the LCDs tested, its general form can be approximated from the summation of the three traces shown in Fig. 3. The three individual color primaries (red, green, and blue) are created by placing color filters over the individual subpixel groups in the LCD pixel grid.[5] The light spectrum output by each color channel is primarily a multiplication of the backlight spectrum by the spectrum of the color filters used in each subpixel. In the example LCD monitor shown in Fig. 3, there is a considerable amount of overlap between each of the three color channels. The amount of overlap varied from monitor to monitor.

The combined spectral results for the 13 LCD monitors tested are shown in Appendix B (Figs. B1, B2, and B3).

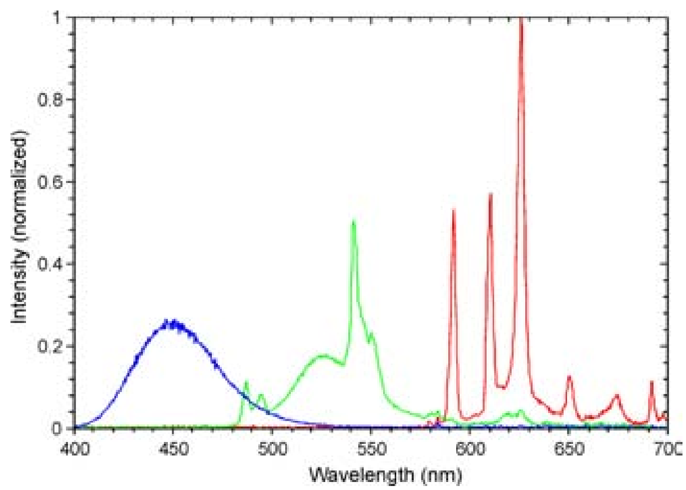

FIGURE 4 — Color spectrum of an example plasma display (PDP08).

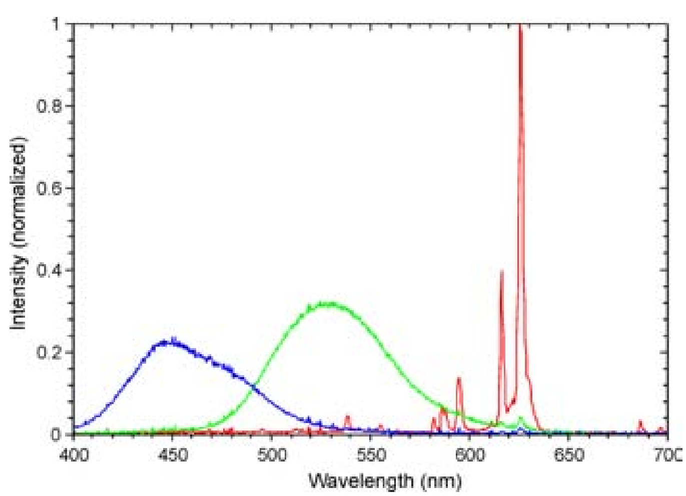

FIGURE 5 — Color spectrum of the example CRT monitor.

A separate graph is provided for each of the three color primaries. There is a lot of similarity between the spectral characteristics of all the LCD monitors; however, some differences occur in the out-of-band rejection (*e.g.*, the amount of green light present in the red color primary) which will probably be related to the quality of color filters used for each of the color primaries.

Figure 4 shows the spectral output of an example plasma display (PDP08). Color plasma displays generate visible light by energizing a gas mixture in each cell so that it emits ultraviolet light rays which in turn causes the phosphor material that coats the inside of each cell to emit visible light. The spectral output of each of the color channels is determined by the phosphor formulation used for each group of subpixels.[6] The blue output has a classic bell-shaped curve centered around 450 nm. The red output is a mixture of several narrow peaks and the green output is a mixture of a bell curve and another major narrow peak.

The combined spectral results for all of the 14 plasma displays tested are shown in Appendix B (Figs. B4, B5, and B6). A separate graph is provided for each of the three color primaries. The color spectrum of the red and blue color primaries are very similar across all the tested plasma displays; however, there is a lot of variation of the spectral response of the green color primary which will probably relate to the formulation of the phosphors used.

Figure 5 shows the spectral output of an example CRT monitor. A previous paper by Woods and Tan[7] reported that 11 tested CRT monitors had almost exactly the same spectral response which suggests that most CRTs use the same phosphor formulation for each of the color primary channels. The blue and green output have a bell-shaped curve whereas the red output is made up of several narrow peaks.

3.2 Anaglyph 3-D glasses results

Figure 4 shows the spectral transmission of an example pair of red-cyan anaglyph glasses. In this example the red filter has a pass band of wavelengths roughly 600–700 nm. The cyan filter has a pass band of wavelengths roughly 550–400 nm. As can be seen in Fig. 4, a little bit of light at the wavelength of around 590 nm will be transmitted through both the red and cyan filters, therefore arriving at both eyes. When this overlap occurs it is another possible source of crosstalk.

All of the anaglyph glasses reported in this paper are listed in Table 2. This list is substantially similar to that reported in Woods and Rourke[2] except that all pairs of glasses have been retested using a more accurate instrument.

The spectral transmission of all the glasses from Table 2 are shown overlaid in Fig. 7 (red filters) and Fig. 8 (cyan filters). It can be seen that there is considerable variation between the spectral response of the various glasses tested. There is some clustering of some of the data, however, this is probably due to some glasses being from the same manufacturer or manufacturing process.

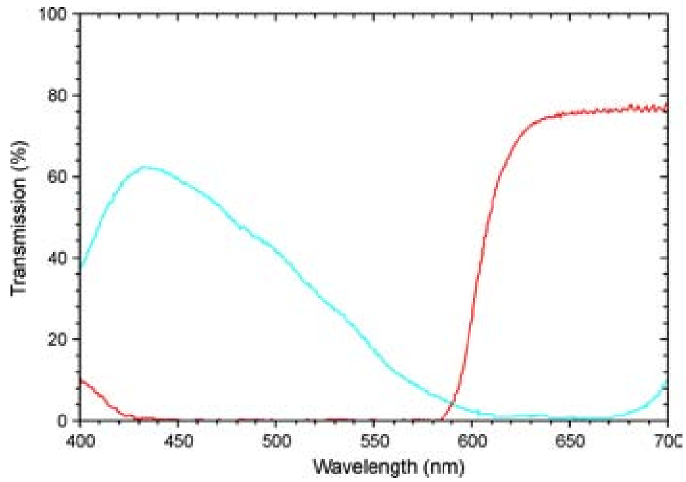

FIGURE 6 — Spectral transmission of an example pair of anaglyph 3-D glasses (3DG16).

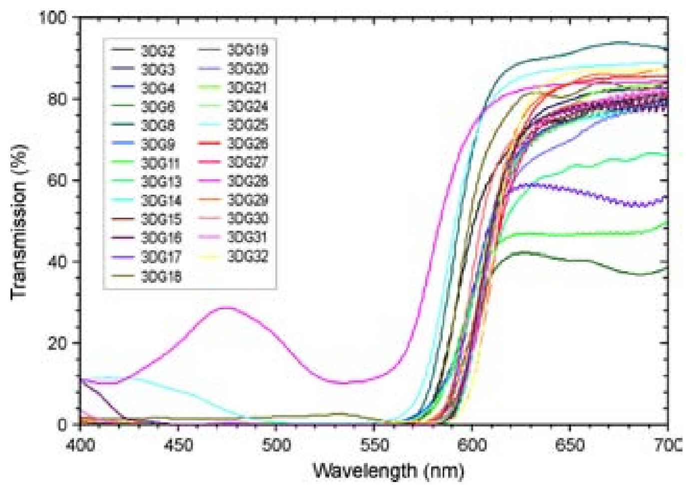

FIGURE 7 — Spectral transmission for all the red filters.

3.3 Crosstalk calculation results

The crosstalk and uncertainty results calculated by the Matlab program for the combination of all displays against all anaglyph glasses are shown in Tables C1 and C2 in Appendix C. For each display/glasses combination, the table lists the percentage crosstalk for the red eye (top left), the percentage crosstalk for the cyan eye (top right), and the overall crosstalk factor for both eyes combined (bottom). The overall crosstalk factor is the sum of the left- and right-eye percentages, and as such is not a percentage. The uncertainty figures are only shown for the overall crosstalk factor. The uncertainty figures were calculated for the individual red and cyan crosstalk but are omitted here due to space limitations.

3.4 Validation test

A first-order validation test was performed to confirm that the results from the crosstalk model were sensible. A set of

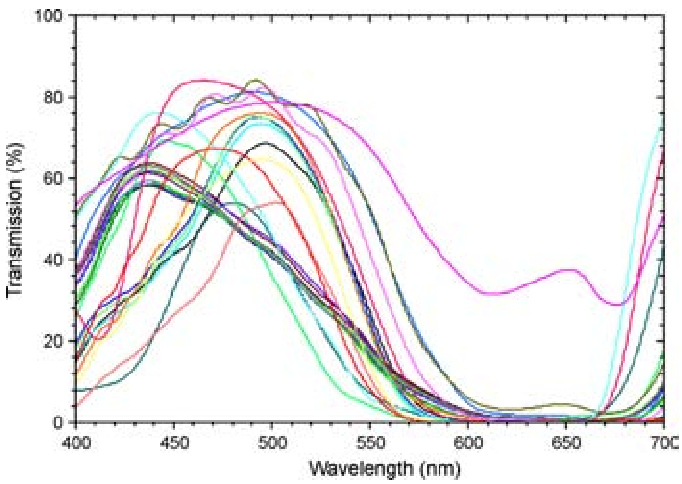

FIGURE 8 — Spectral transmission for all the cyan filters.

TABLE 2 — Subjective testing of anaglyph glasses and comparison with calculated results. Lines join matching entries.

Red filter			Cyan		
Subjective	Calculated		Subjective	Calculated	
Glasses	Glasses	Cross-talk	Glasses	Glasses	Cross-talk
3DG32	3DG32	14.4	3DG26	3DG26	3.6
3DG26	3DG26	14.8	3DG30	3DG32	3.8
3DG3	3DG3	14.8	3DG32	3DG30	3.8
3DG31	3DG31	15.4	3DG24	3DG24	4.0
3DG19	3DG16	15.6	3DG14	3DG14	4.0
3DG16	3DG19	16.0	3DG4	3DG4	4.0
3DG21	3DG21	16.2	3DG2	3DG2	4.1
3DG15	3DG15	16.2	3DG27	3DG27	4.1
3DG27	3DG27	16.4	3DG8	3DG8	4.3
3DG20	3DG20	16.9	3DG25	3DG25	4.3
3DG29	3DG29	17.3	3DG29	3DG29	4.4
3DG30	3DG30	19.7	3DG31	3DG31	4.7
3DG17	3DG17	20.0	3DG11	3DG11	4.9
3DG6	3DG6	20.6	3DG6	3DG6	4.9
3DG14	3DG24	22.4	3DG20	3DG17	5.3
3DG24	3DG14	22.8	3DG17	3DG20	5.4
3DG9	3DG9	22.8	3DG3	3DG3	5.5
3DG4	3DG4	23.4	3DG19	3DG9	5.7
3DG2	3DG2	25.6	3DG21	3DG19	5.7
3DG11	3DG11	27.0	3DG16	3DG21	5.8
3DG8	3DG8	28.9	3DG15	3DG16	5.8
3DG18	3DG18	35.1	3DG9	3DG15	5.8
3DG25	3DG25	37.8	3DG18	3DG18	6.1
3DG28	3DG28	112.8	3DG28	3DG28	15.1

test images were viewed on a CRT monitor and subjectively ranked in order of increasing crosstalk. The results of the subjective ranking were then compared with the crosstalk ranking generated by the MATLAB program and this is shown in Table 2.

As can be seen from the table, the subjective ranking agrees extremely well with the calculated results, which provides some confidence in the validity of the crosstalk calculation results. Two of the differences occurred where the crosstalk percentage difference was just 0.1, and two differences occurred where the crosstalk percentage difference was 0.4. Crosstalk differences of 0.1 and 0.4 are very small and are hard to discern by the naked eye.

4 Discussion

Crosstalk in anaglyph images acts to degrade the 3-D image quality by making them hard to fuse. One important way to optimize the quality of anaglyph 3-D images is therefore to minimize the presence of crosstalk. In most circumstances, the easiest way to minimize crosstalk would be with the choice of anaglyph 3-D glasses, but in some circumstances it may also be possible to choose different display monitors. This project aims to highlight possible low-crosstalk combinations so crosstalk can be reduced.

Across all of the displays, the LCD monitors had the lowest overall crosstalk, both from an average (18.6) and also a global minimum (7.0) perspective. The plasma displays were very close behind with an average overall crosstalk of 18.6 and global minimum of 8.1. The CRT had much worse anaglyph crosstalk with an average overall crosstalk of 27.0 and global minimum of 18.2. On average, the CRT had 45% more crosstalk than the LCD and plasma displays.

As cited earlier, there is a reasonable amount of variation of the color spectrum across all LCD monitors and across all plasma displays. Similarly, there is a fairly large variation in overall crosstalk factor across all of the LCD monitors and all of the plasma displays. For example, the LCD monitor with the highest crosstalk factors (LCD04) only performs marginally better than a CRT, and the plasma display with the highest crosstalk factors (PDP02) had slightly worse performance than a CRT.

The best performing LCD monitor was LCD14 which provided an average crosstalk factor of only 13.8 and achieved the lowest crosstalk factor across all displays of 7.0 (when combined with glasses 3DG32). The best performing plasma display was the PDP12 with an average crosstalk factor of 11.9 which achieved the third lowest crosstalk factor across all plasma displays of 8.1 (when used with glasses 3DG13).

The worst pair of anaglyph glasses across all displays by far was 3DG28 – the ink-jet-printed transparency filters. This is not an unexpected result since these filters have such poor performance in the out-of-band wavelengths and very poor contrast.

The choice of best glasses depends upon which display is being considered. For the LCD monitors, 3DG32, 3DG26, and 3DG13 usually had the lowest overall crosstalk (all were within the uncertainty limits of each other). For the plasma displays, 3DG30, 3DG13, and 3DG32 usually had the lowest overall crosstalk (within the uncertainty limits). For the CRT case, the best glasses were 3DG32, 3DG26, and 3DG13. It is interesting to note that the "cyan" filters of 3DG13 and 3DG26 have a more blue appearance than those of 3DG30 and 3DG32 that have a more cyan appearance. These differences may have some effect on color perception which is discussed below.

As can be seen in Tables C1 and C2, red crosstalk is usually significantly greater than cyan crosstalk – on average almost four times greater. Red crosstalk usually therefore dominates the overall crosstalk value. This can be attributed to the shape of the spectral curves for the display and glasses, but will also be due to the fact that the green channel is usually much brighter than the red channel.

It is usually possible to obtain a slightly lower overall crosstalk figure for a particular display by mixing and matching filters from different glasses; however, the improvement achieved is usually less than the calculated overall uncertainty value.

It is worth mentioning that even a perfect filter (one that transmits 100% of light in the desired wavelength domain and 0% outside it) would still have crosstalk if the display's color channels overlap in the spectral domain (as most displays do).

Three further items are worth considering. First, intensity. If the filter cuts out most of the light, the image will be very dim and hard to see. Lower light levels also make the effect of even small ghosting levels proportionally greater than they might otherwise be. A brightness imbalance between left and right eye can also result in the Pulfrich effect[8] whereby horizontal motion can be interpreted as binocular depth, which is generally undesirable. Brightness levels and imbalance have not been considered in this paper.

Second, color perception. Truly full-color stereoscopic images are not possible with anaglyphs, but a properly constructed anaglyph using complimentary colors can approximate a full-color image. This distorted color image is usually referred to as a "pseudo-color anaglyph" or a "polychromatic anaglyph" as opposed to a "full-color anaglyph" (which is not possible). If a non-complimentary combination is used (*e.g.*, red/blue or red/green), pseudo-color anaglyphs are impossible because a large portion of the visible spectrum is missing. The overall image may also be darker. This paper has only considered red/cyan anaglyphs, although it is sometimes hard to draw a line between what is classified as a cyan filter and what is classified as a blue filter.

Third, color balance and color temperature. Most monitors allow the color balance or color temperature of the display to be adjusted. This allows the user to change the relative intensities of the three color channels (but not the spectral output of each color channel). We have found that such adjustments do affect the results of the crosstalk calculations; however, as yet we have not used this knowledge to choose an optimum color balance, or performed any validation experiments to confirm whether the simulation of color balance changes matches human perception. For the purposes of this study, the default color profiles were used for each monitor.

5 Conclusion

Although there are a range of stereoscopic display technologies available that produce much better 3-D image quality than the anaglyph 3-D method, the anaglyph remains widely used because of its simplicity, low cost, and compatibility with all full-color displays. This paper highlights one particular way of improving the image quality of anaglyph 3-D images specifically relating to spectral crosstalk.

This study has revealed that crosstalk in anaglyphic 3-D images can be minimized by the appropriate choice of anaglyphic 3-D glasses. The study has revealed that there can be considerable variation in the amount of crosstalk present when an anaglyphic 3-D display is viewed with different anaglyphic 3-D glasses.

The study has also revealed that there is considerable variation in the amount of anaglyphic crosstalk exhibited by different displays. For example, on average CRT monitors exhibit approximately 45% more crosstalk than LCD monitors and plasma displays.

An anaglyphic crosstalk calculation algorithm has been developed that appears to work well and generates outputs that agree well with subjective assessments of anaglyphic 3-D crosstalk.

It should be noted that the results of this paper are not intended to be a leader board of one glasses manufacturer versus another – we have not tested all glasses from all manufacturers, nor have we tested a large sample of each manufacturers glasses. This paper does, however, highlight that there is significant variation between different anaglyph 3-D glasses and displays. Further crosstalk optimization may be possible by using the anaglyphic crosstalk calculation algorithm and working with 3-D glasses manufacturers.

Acknowledgments

We would like to thank the multitude of companies and individuals who lent LCD monitors and plasma displays for testing.[3,9] We also wish to thank iVEC (the hub of advanced computing in Western Australia) and Jumbo Vision International for their support of the plasma displays phase of this project.

References

1 R Zone, "Good old fashion anaglyph: High tech tools revive a classic format in spy kids 3-D," *Stereo World* **29**, No. 5, 11–13 and 46 (2002–2003).

2 A J Woods and T Rourke, "Ghosting in anaglyphic stereoscopic images," *Stereoscopic Displays and Virtual Reality Systems XI, Proc SPIE* **5291**, 354–365 (2004).

3 K S Karvinen and A J Woods, "The compatibility of plasma displays with stereoscopic visualization," *Technical Report CMST2007-04* (Curtin University of Technology, Australia, 2007).

4 CIE, *Commission Internationale de l'Eclairage Proceedings* (Cambridge University Press, 1932).
5 B A Wandell and L D Silverstein, "Digital color reproduction," *The Science of Color* (Elsevier, 2003), pp. 296.
6 H Uchiike and T Hirakawa, "Color plasma displays," *Proc IEEE* **90**, Issue 4, 533–539 (2002).
7 A J Woods and S S L Tan, "Characterizing sources of ghosting in time-sequential stereoscopic video displays," *Stereoscopic Displays and Virtual Reality Systems IX, Proc SPIE* **4660**, 66–77 (2002).
8 C Pulfrich, "Die Stereoskopie im Dienste der isochromem und herterochromen Photometrie," *Naturwissenschaft* **10**, 553–564 (1922).
9 K L Yuen, "Compatibility of LCD monitors with stereoscopic display methods," *Undergraduate Student Project Report* (Curtin University of Technology, 2006).

Appendix A: Red/cyan anaglyph glasses

Appendix B: Spectral results for all tested LCD monitors and plasma displays

The figures below show the spectral results for each color channel of all tested LCD monitors and plasma displays. Figure B1 is normalized on the average value between 450 and 455 nm. Figures B2 and B3 are normalized on the peak value. Figures B4–B6 are normalized on the area under the

TABLE A1 — Red/cyan anaglyphic 3-D glasses measured.

Glasses Number	Name	Other information on glasses
3DG 2	IMAX/OMNIMAX	"Fujitsu presentation of "We are born of stars"; © IMAX Systems Corp., 1986; Made in USA by Theatric Support, Studio City, California."
3DG 3	National Geographic	Distributed with August 1998 edition of National Geographic Magazine
3DG 4	Sports Illustrated	Distributed with Winter 2000 edition of Sports Illustrated magazine (US edition). "MFGD by Theatric Support."
3DG 6	3D Greets	Attached to a pseudo-color anaglyph postcard of a Tiger.
3DG 8	Spectacles	"Theatric Support, Studio City CA" Plastic hard-framed spectacles purchased from Reel-3D.
3DG 9	Bugs!	From *Bugs!* magazine series
3DG 11	[no name]	[no identification or writing on glasses – white cardboard]
3DG 13	Toyota	"Seeing is believing – The New Toyota Camry" advertising flyer.
3DG 14	Reel 3D	#1 Purchased from Reel-3D – apparently made by Theatric Support.
3DG 15	Reel 3D	#2 Purchased from Reel-3D.
3DG 16	Freddy's Dead	"*The Final Nightmare*; New Line Cinema 1991" Distributed at showings of the movie "Freddy's Dead: The Final Nightmare"
3DG 17	3D Video Glasses	"© 1982 3D Video Corp., N. Hollywood, California; for use with 3D Video electronically processed TV programs"
3DG 18	Rhino Home Video	"*Cat Women of the Moon*", "*Robot Monster*" & "*The Mask*"
3DG 19	DDD	"www.ddd3d.com Dynamic Digital Depth". Supplied by American Paper Optics.
3DG 20	ABC	"96/97 new season premiere; http://abc.com"
3DG 21	Optic Boom	"A DDD Product; ddd.com"
3DG 24	Studio 3D	"Stereoscopic imaging; www.studio3d.com"
3DG 25	Sports Illustrated Australian Edition	Distributed with March 2000 edition of Sports Illustrated magazine (Australian edition).
3DG 26	Substance Comic	Distributed with "3-D Substance #2" Comic, by Jack C. Harris and Steve Ditko and The 3-D Zone. ©1991.
3DG 27	Deep Vision 3D of Hollywood	"For Deep Vision 3-D TV"
3DG 28	Canon ink	Canon Ink (BCI-3e C/M/Y) printed on inkjet transparency sheet
3DG 29	Spy Kids 3D	"© 2003 Miramax Film Corp.; www.spykids.com; Troublemaker Studios; Dimension Films; Manufactured by Playwerks Inc., USA" As supplied at movie theatres.
3DG 30	The Adventures of Shark Boy and Lava Girl	"© 2004 Miramax Film Corp.; Troublemaker Studios; Dimension Films; Columbia Pictures; Playwerks Premium Solutions" As supplied at movie theatres.
3DG 31	Shrek 3-D	Glasses blank white. As supplied with the Shrek 3-D DVD Region 4
3DG 32	World 3-D Film Expo	"WORLD 3-D FILM EXPO is a SubuCat Productions presentation www.sabucat .com" "REAL 3D is a trademark of and glasses made in U.S.A. by Dimension 3" As supplied with the World 3-D Film Expo Souvenir Book.

Note: Although a wide selection of glasses was tested, generally only a single pair of glasses of each particular style/brand was sampled. As such, due to manufacturing variations or experimental error, the results provided in this paper should not be considered to be representative of all glasses of that particular style/brand.

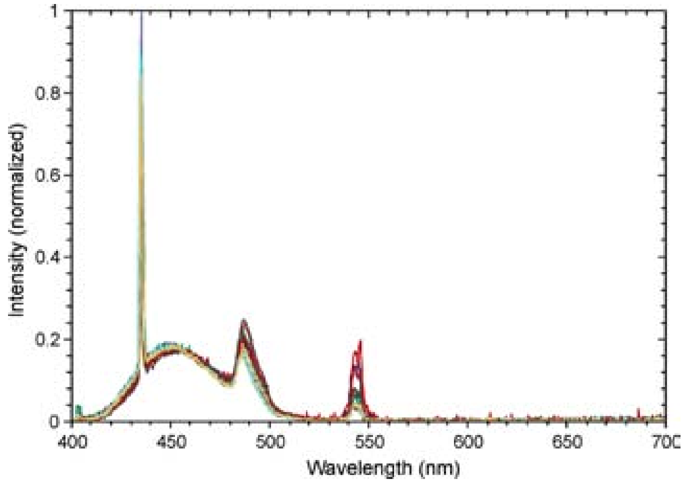

FIGURE B1 — Blue-color-primary spectral output for 13 LCD monitors.

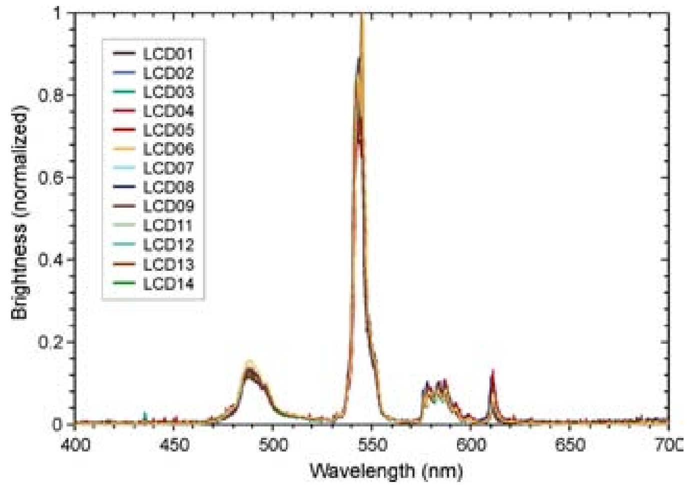

FIGURE B2 — Green-color-primary spectral output for 13 LCD monitors.

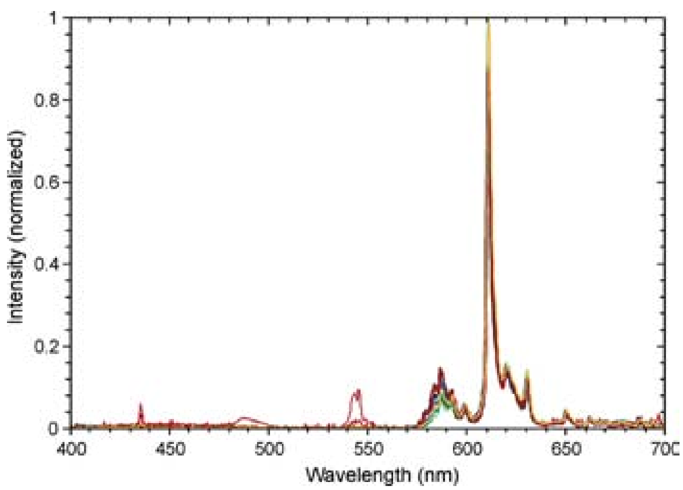

FIGURE B3 — Red-color-primary spectral output for 13 LCD monitors.

curve. These normalizations were chosen so as to more easily reveal the similarities and differences between the various traces.

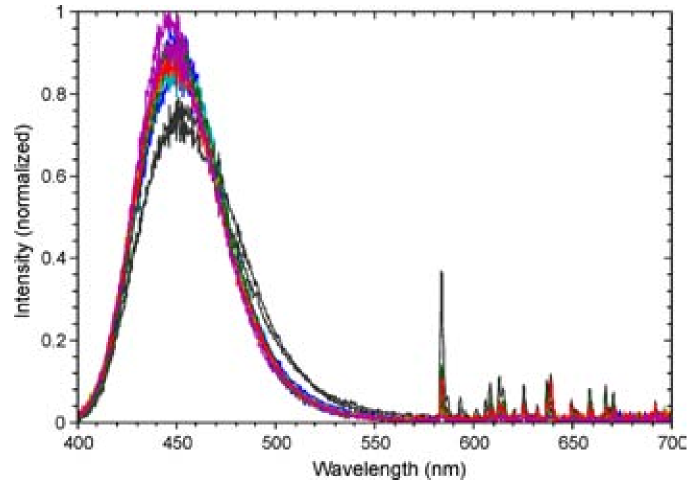

FIGURE B4 — Blue-color-primary spectral output for 14 plasma displays.

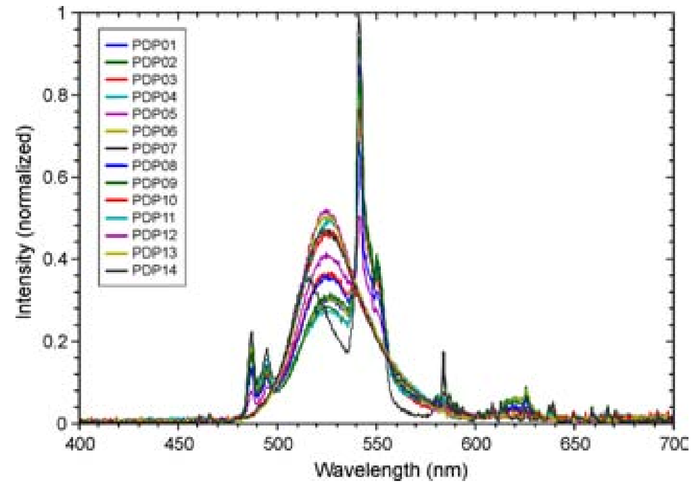

FIGURE B5 — Green-color-primary spectral output for 14 plasma displays.

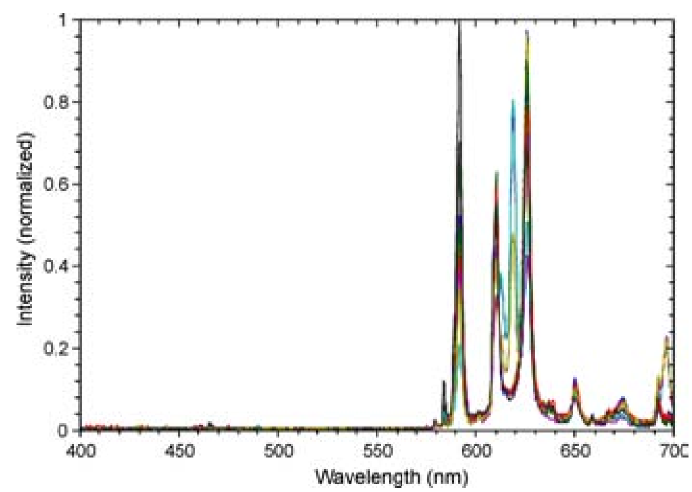

FIGURE B6 — Red-color-primary spectral output for 14 plasma displays.

Appendix C: Crosstalk calculation results for LCD monitors and plasma displays

The following tables contain the results from the crosstalk calculation program. Every combination of anaglyph glasses and display has been calculated. The lowest overall crosstalk combinations are highlighted in bright green and the worst overall crosstalk results are highlighted in orange. Overall crosstalk results of less than 15 have been highlighted in light green. Red crosstalk percentages less than nine have been highlighted in pink, and cyan crosstalk percentages less than 1.5 have been highlighted in cyan. These threshold figures do not have any significance apart from allowing us to highlight the lower crosstalk results.

TABLE C1 — Crosstalk calculation results for the LCD and CRT monitors. The top left cell of each combination is red crosstalk %, the top right cell of each combination is cyan crosstalk %, and the bottom cell of each combination is the overall crosstalk factor and uncertainty.

	LCD01	LCD02	LCD03	LCD04	LCD05	LCD06	LCD07	LCD08	LCD09	LCD11	LCD12	LCD13	LCD14	CRT
3DG02	17.7 / 0.9	15.9 / 0.9	17.1 / 0.6	20.1 / 7.8	23.8 / 2.6	14.2 / 0.8	17.8 / 1.0	24.0 / 1.5	16.1 / 1.7	13.8 / 1.4	16.5 / 1.2	15.3 / 0.4	14.1 / 0.6	25.6 / 4.1
	18.6 ± 1.6	16.8 ± 1.5	17.7 ± 1.6	27.9 ± 2.4	26.5 ± 2.4	15.0 ± 1.3	18.8 ± 1.7	25.6 ± 2.3	17.8 ± 1.6	15.2 ± 1.3	17.8 ± 1.6	15.7 ± 1.4	14.8 ± 1.3	29.7 ± 1.4
3DG03	8.3 / 3.5	7.6 / 3.3	10.7 / 3.0	9.6 / 9.7	15.4 / 5.4	7.8 / 3.4	9.6 / 3.5	16.3 / 4.3	10.1 / 5.0	7.6 / 3.8	9.4 / 4.2	7.0 / 2.4	6.6 / 2.8	14.8 / 5.5
	11.7 ± 1.0	10.9 ± 1.0	13.6 ± 1.2	19.2 ± 1.7	20.8 ± 1.9	11.3 ± 1.0	13.1 ± 1.2	20.6 ± 1.8	15.0 ± 1.4	11.4 ± 1.0	13.6 ± 1.2	9.4 ± 0.8	9.5 ± 0.8	20.3 ± 0.9
3DG04	16.0 / 0.7	14.4 / 0.7	15.9 / 0.5	18.0 / 7.6	22.2 / 2.4	13.0 / 0.7	16.5 / 0.9	22.8 / 1.4	15.3 / 1.4	12.8 / 1.3	15.4 / 1.1	13.9 / 0.3	12.9 / 0.5	23.4 / 4.0
	16.7 ± 1.5	15.1 ± 1.3	16.4 ± 1.5	25.7 ± 2.2	24.7 ± 2.2	13.7 ± 1.2	17.4 ± 1.6	24.1 ± 2.1	16.8 ± 1.5	14.1 ± 1.2	16.5 ± 1.5	14.2 ± 1.3	13.4 ± 1.2	27.5 ± 1.3
3DG06	12.0 / 2.6	10.8 / 2.4	13.1 / 2.1	13.8 / 9.0	18.8 / 4.4	10.2 / 2.5	12.5 / 2.7	19.2 / 3.3	11.9 / 3.8	9.7 / 2.9	11.9 / 3.2	9.9 / 1.7	9.3 / 2.0	20.6 / 4.9
	14.6 ± 1.3	13.2 ± 1.2	15.2 ± 1.4	22.8 ± 2.0	23.2 ± 2.1	12.7 ± 1.1	15.2 ± 1.4	22.5 ± 2.0	15.8 ± 1.4	12.7 ± 1.1	15.0 ± 1.3	11.6 ± 1.0	11.4 ± 1.0	25.5 ± 1.2
3DG08	20.4 / 1.6	18.3 / 1.7	19.1 / 1.5	23.2 / 8.2	26.2 / 3.3	16.2 / 1.8	20.3 / 1.9	26.3 / 2.4	17.9 / 2.6	15.8 / 2.5	18.7 / 2.3	17.9 / 1.1	16.5 / 1.5	28.9 / 4.3
	22.1 ± 1.9	20.1 ± 1.8	20.5 ± 1.8	31.4 ± 2.7	29.5 ± 2.6	17.9 ± 1.6	22.2 ± 2.0	28.7 ± 2.5	20.5 ± 1.8	18.3 ± 1.6	21.0 ± 1.9	19.0 ± 1.7	18.0 ± 1.6	33.1 ± 1.5
3DG09	15.2 / 3.5	13.6 / 3.2	15.3 / 2.8	17.1 / 9.7	21.5 / 5.4	12.4 / 3.2	15.8 / 3.5	22.1 / 4.3	14.9 / 5.0	12.2 / 3.5	14.8 / 4.1	13.2 / 2.3	12.2 / 2.7	22.8 / 5.7
	18.7 ± 1.6	16.8 ± 1.5	18.1 ± 1.6	26.8 ± 2.3	26.9 ± 2.4	15.7 ± 1.4	19.2 ± 1.7	26.4 ± 2.3	19.9 ± 1.8	15.7 ± 1.4	18.9 ± 1.7	15.5 ± 1.4	14.9 ± 1.3	28.5 ± 1.3
3DG10	24.8 / 0.7	22.2 / 0.8	22.4 / 0.5	27.7 / 7.3	29.8 / 2.3	19.3 / 0.8	24.0 / 1.0	29.7 / 1.4	21.1 / 1.4	18.8 / 1.7	22.0 / 1.3	21.9 / 0.3	20.1 / 0.6	32.2 / 3.4
	25.5 ± 2.2	23.0 ± 2.0	22.9 ± 2.0	35.0 ± 3.1	32.1 ± 2.9	20.1 ± 1.8	25.1 ± 2.2	31.2 ± 2.7	22.5 ± 2.0	20.5 ± 1.8	23.2 ± 2.1	22.2 ± 2.0	20.8 ± 1.8	35.6 ± 1.6
3DG11	18.4 / 2.5	16.4 / 2.3	17.6 / 2.0	20.7 / 8.9	24.3 / 4.3	14.6 / 2.4	18.2 / 2.6	24.5 / 3.2	16.6 / 3.7	14.1 / 2.8	16.9 / 3.1	15.8 / 1.6	14.6 / 2.0	27.0 / 4.9
	20.9 ± 1.8	18.7 ± 1.6	19.6 ± 1.7	29.6 ± 2.6	28.6 ± 2.5	17.0 ± 1.5	20.8 ± 1.9	27.7 ± 2.4	20.3 ± 1.8	17.0 ± 1.5	19.9 ± 1.8	17.4 ± 1.5	16.6 ± 1.5	31.8 ± 1.5
3DG13	8.1 / 0.9	7.5 / 1.0	10.5 / 0.7	9.4 / 7.5	15.3 / 2.5	7.7 / 1.0	9.4 / 1.2	16.1 / 1.6	9.8 / 1.6	7.5 / 1.9	9.2 / 1.5	6.8 / 0.5	6.4 / 0.8	15.5 / 3.5
	9.0 ± 0.8	8.5 ± 0.8	11.3 ± 1.0	16.9 ± 1.5	17.8 ± 1.6	8.7 ± 0.8	10.6 ± 1.0	17.8 ± 1.6	11.5 ± 1.0	9.3 ± 0.8	10.7 ± 1.0	7.3 ± 0.7	7.3 ± 0.7	19.1 ± 0.9
3DG14	15.5 / 0.7	13.9 / 0.7	15.5 / 0.5	17.5 / 7.6	21.8 / 2.4	12.7 / 0.7	16.0 / 0.9	22.3 / 1.4	15.0 / 1.4	12.4 / 1.3	15.0 / 1.1	13.4 / 0.3	12.4 / 0.5	22.8 / 4.0
	16.2 ± 1.4	14.7 ± 1.3	16.0 ± 1.4	25.1 ± 2.2	24.2 ± 2.2	13.3 ± 1.2	16.9 ± 1.5	23.7 ± 2.1	16.4 ± 1.5	13.7 ± 1.2	16.1 ± 1.4	13.7 ± 1.2	13.0 ± 1.2	26.8 ± 1.2
3DG15	9.4 / 3.9	8.6 / 3.7	11.4 / 3.4	10.8 / 10.1	16.4 / 5.9	8.5 / 3.9	10.5 / 4.0	17.2 / 4.8	10.7 / 5.5	8.3 / 4.2	10.1 / 4.7	7.9 / 2.8	7.4 / 3.3	16.2 / 5.8
	13.3 ± 1.2	12.3 ± 1.1	14.8 ± 1.3	20.9 ± 1.8	22.3 ± 2.0	12.4 ± 1.1	14.5 ± 1.3	22.0 ± 1.9	16.3 ± 1.5	12.5 ± 1.1	14.8 ± 1.3	10.7 ± 0.9	10.7 ± 1.0	22.1 ± 1.0
3DG16	8.4 / 3.9	7.8 / 3.7	10.8 / 3.4	9.8 / 10.1	15.6 / 5.9	7.9 / 3.9	9.6 / 4.0	16.4 / 4.8	10.0 / 5.5	7.7 / 4.3	9.4 / 4.7	7.1 / 2.8	6.7 / 3.3	15.6 / 5.8
	12.4 ± 1.1	11.5 ± 1.0	14.2 ± 1.3	19.9 ± 1.7	21.5 ± 1.9	11.9 ± 1.0	13.7 ± 1.2	21.2 ± 1.9	15.6 ± 1.4	11.9 ± 1.1	14.2 ± 1.3	9.9 ± 0.9	10.0 ± 0.9	21.4 ± 1.0
3DG17	11.5 / 3.2	10.4 / 3.0	12.8 / 2.7	13.3 / 9.4	18.4 / 5.0	9.9 / 3.1	12.1 / 3.2	18.8 / 4.0	11.7 / 4.6	9.5 / 3.5	11.6 / 3.8	9.6 / 2.1	9.0 / 2.6	20.0 / 5.3
	14.7 ± 1.3	13.4 ± 1.2	15.5 ± 1.4	22.7 ± 2.0	23.5 ± 2.1	13.0 ± 1.1	15.4 ± 1.4	22.8 ± 2.0	16.3 ± 1.5	13.0 ± 1.2	15.4 ± 1.4	11.7 ± 1.0	11.5 ± 1.0	25.3 ± 1.2
3DG18	27.6 / 3.9	24.3 / 3.6	24.4 / 3.4	29.7 / 10.1	31.9 / 5.9	21.0 / 3.8	26.3 / 3.9	32.1 / 4.8	24.3 / 5.5	20.5 / 4.1	23.9 / 4.6	24.3 / 2.7	22.3 / 3.2	35.1 / 6.1
	31.5 ± 2.7	27.9 ± 2.4	27.8 ± 2.4	39.8 ± 3.5	37.7 ± 3.3	24.8 ± 2.2	30.2 ± 2.7	36.9 ± 3.2	29.8 ± 2.6	24.6 ± 2.2	28.5 ± 2.5	27.0 ± 2.4	25.4 ± 2.2	41.2 ± 1.9
3DG19	9.0 / 3.8	8.3 / 3.6	11.1 / 3.3	10.4 / 10.0	16.1 / 5.7	8.3 / 3.8	10.2 / 3.8	16.9 / 4.6	10.5 / 5.4	8.1 / 4.1	10.0 / 4.5	7.6 / 2.6	7.2 / 3.1	16.0 / 5.7
	12.8 ± 1.1	11.9 ± 1.1	14.4 ± 1.3	20.4 ± 1.8	21.8 ± 2.0	12.1 ± 1.1	14.1 ± 1.3	21.6 ± 1.9	15.9 ± 1.4	12.2 ± 1.1	14.5 ± 1.3	10.3 ± 0.9	10.3 ± 0.9	21.7 ± 1.0
3DG20	9.6 / 3.4	8.8 / 3.2	11.5 / 2.8	11.1 / 9.6	16.7 / 5.2	8.7 / 3.3	10.7 / 3.4	17.4 / 4.2	10.8 / 4.8	8.4 / 3.7	10.3 / 4.0	8.1 / 2.3	7.6 / 2.7	16.9 / 5.4
	13.0 ± 1.1	12.0 ± 1.1	14.4 ± 1.3	20.7 ± 1.8	21.9 ± 2.0	12.0 ± 1.1	14.1 ± 1.3	21.6 ± 1.9	15.6 ± 1.4	12.1 ± 1.1	14.4 ± 1.3	10.4 ± 0.9	10.4 ± 0.9	22.3 ± 1.0
3DG21	9.4 / 3.8	8.6 / 3.6	11.4 / 3.3	10.8 / 10.0	16.4 / 5.7	8.5 / 3.8	10.5 / 3.9	17.2 / 4.7	10.8 / 5.4	8.3 / 4.2	10.2 / 4.6	7.9 / 2.7	7.5 / 3.2	16.2 / 5.8
	13.2 ± 1.2	12.2 ± 1.1	14.7 ± 1.3	20.8 ± 1.8	22.2 ± 2.0	12.4 ± 1.1	14.4 ± 1.3	21.9 ± 1.9	16.2 ± 1.4	12.5 ± 1.1	14.8 ± 1.3	10.6 ± 0.9	10.6 ± 0.9	21.9 ± 1.0
3DG24	15.2 / 0.7	13.6 / 0.7	15.3 / 0.5	17.1 / 7.6	21.5 / 2.4	12.4 / 0.6	15.7 / 0.8	22.1 / 1.3	14.8 / 1.3	12.2 / 1.3	14.8 / 1.0	13.1 / 0.2	12.2 / 0.5	22.4 / 4.0
	15.8 ± 1.4	14.3 ± 1.3	15.8 ± 1.4	24.7 ± 2.2	23.9 ± 2.1	13.1 ± 1.1	16.5 ± 1.5	23.4 ± 2.1	16.1 ± 1.4	13.4 ± 1.2	15.8 ± 1.4	13.4 ± 1.2	12.6 ± 1.1	26.3 ± 1.2
3DG25	27.8 / 1.6	25.2 / 1.7	24.9 / 1.5	31.2 / 8.1	32.6 / 3.3	21.5 / 1.8	27.2 / 1.9	32.8 / 2.4	23.6 / 2.6	21.4 / 2.6	24.6 / 2.3	25.4 / 1.1	23.1 / 1.5	37.8 / 4.3
	29.4 ± 2.6	26.9 ± 2.3	26.3 ± 2.3	39.3 ± 3.4	35.9 ± 3.2	23.3 ± 2.0	29.1 ± 2.6	35.1 ± 3.1	26.2 ± 2.3	24.0 ± 2.1	26.9 ± 2.4	26.5 ± 2.3	24.6 ± 2.2	42.1 ± 1.9
3DG26	8.4 / 0.5	7.8 / 0.7	10.7 / 0.4	9.5 / 7.3	15.3 / 2.2	7.9 / 0.6	9.8 / 0.8	16.4 / 1.3	10.6 / 1.2	7.8 / 1.4	9.7 / 1.0	7.2 / 0.2	6.8 / 0.5	14.8 / 3.6
	8.9 ± 0.8	8.4 ± 0.8	11.2 ± 1.0	16.8 ± 1.5	17.5 ± 1.6	8.5 ± 0.8	10.6 ± 1.0	17.7 ± 1.6	11.8 ± 1.1	9.2 ± 0.8	10.7 ± 1.0	7.4 ± 0.7	7.2 ± 0.7	18.4 ± 0.8
3DG27	10.3 / 1.0	9.5 / 0.9	12.0 / 0.7	11.8 / 7.8	17.2 / 2.7	9.2 / 0.9	11.5 / 1.1	18.1 / 1.6	11.8 / 1.8	9.1 / 1.5	11.1 / 1.3	8.9 / 0.4	8.3 / 0.7	16.4 / 4.1
	11.3 ± 1.0	10.4 ± 0.9	12.7 ± 1.1	19.6 ± 1.7	19.9 ± 1.8	10.1 ± 0.9	12.6 ± 1.1	19.8 ± 1.8	13.5 ± 1.2	10.5 ± 0.9	12.5 ± 1.1	9.3 ± 0.8	9.0 ± 0.8	20.5 ± 0.9
3DG28	92.7 / 14.5	84.5 / 15.0	78.7 / 15.7	97.0 / 19.5	87.5 / 18.1	70.9 / 17.2	85.7 / 15.4	87.9 / 17.1	74.2 / 18.9	71.1 / 17.4	75.5 / 17.8	90.8 / 13.0	81.8 / 14.6	112.8 / 15.1
	107.2 ± 9.2	99.5 ± 8.6	94.4 ± 8.2	116.5 ± 10.0	105.5 ± 9.2	88.1 ± 7.6	101.1 ± 8.8	105.1 ± 9.1	93.1 ± 8.1	88.5 ± 7.6	93.3 ± 8.1	103.8 ± 9.0	96.5 ± 8.3	127.9 ± 5.7
3DG29	10.9 / 1.6	9.9 / 1.5	12.4 / 1.3	12.5 / 8.2	17.8 / 3.3	9.6 / 1.5	11.9 / 1.7	18.5 / 2.3	11.9 / 2.5	9.3 / 2.1	11.4 / 2.0	9.3 / 0.9	8.7 / 1.2	17.3 / 4.4
	12.5 ± 1.1	11.5 ± 1.0	13.7 ± 1.2	20.7 ± 1.8	21.1 ± 1.9	11.1 ± 1.0	13.6 ± 1.2	20.8 ± 1.8	14.4 ± 1.3	11.4 ± 1.0	13.5 ± 1.2	10.2 ± 0.9	9.9 ± 0.9	21.6 ± 1.0
3DG30	11.3 / 0.5	10.3 / 0.6	12.7 / 0.4	13.1 / 7.4	18.3 / 2.2	9.8 / 0.5	12.0 / 0.7	18.7 / 1.2	11.7 / 1.2	9.4 / 1.3	11.5 / 0.9	9.4 / 0.2	8.9 / 0.4	19.7 / 3.8
	11.8 ± 1.0	10.9 ± 1.0	13.1 ± 1.2	20.5 ± 1.8	20.5 ± 1.8	10.4 ± 0.9	12.8 ± 1.2	19.9 ± 1.8	12.9 ± 1.2	10.7 ± 1.0	12.4 ± 1.1	9.6 ± 0.9	9.3 ± 0.8	23.4 ± 1.1
3DG31	8.7 / 1.9	8.0 / 1.7	11.0 / 1.4	10.1 / 8.5	15.8 / 3.7	8.1 / 1.7	9.9 / 1.9	16.7 / 2.6	10.4 / 3.0	7.9 / 2.1	9.7 / 2.3	7.4 / 1.1	7.0 / 1.4	15.4 / 4.7
	10.7 ± 0.9	9.8 ± 0.9	12.4 ± 1.1	18.6 ± 1.6	19.5 ± 1.8	9.8 ± 0.9	11.9 ± 1.1	19.3 ± 1.7	13.4 ± 1.2	10.0 ± 0.9	12.0 ± 1.1	8.5 ± 0.8	8.4 ± 0.7	20.1 ± 0.9
3DG32	8.1 / 0.6	7.5 / 0.7	10.6 / 0.4	9.2 / 7.5	15.1 / 2.3	7.7 / 0.6	9.6 / 0.8	16.2 / 1.3	10.4 / 1.2	7.7 / 1.3	9.5 / 1.0	7.0 / 0.2	6.6 / 0.5	14.4 / 3.8
	8.7 ± 0.8	8.2 ± 0.7	11.0 ± 1.0	16.7 ± 1.5	17.4 ± 1.6	8.3 ± 0.7	10.4 ± 0.9	17.4 ± 1.6	11.6 ± 1.1	9.0 ± 0.8	10.4 ± 0.9	7.2 ± 0.6	7.0 ± 0.6	18.2 ± 0.8

TABLE C2 — Crosstalk calculation results for the plasma displays. The top left cell of each combination is red crosstalk %, the top right cell of each combination is cyan crosstalk %, and the bottom cell of each combination is the overall crosstalk factor and uncertainty.

	PDP01	PDP02	PDP03	PDP04	PDP05	PDP06	PDP07
3DG02	14.5 / 1.2	24.1 / 1.1	9.5 / 2.2	15.2 / 2.5	10.8 / 2.3	17.4 / 1.6	13.2 / 1.5
	15.7 ± 1.4	25.2 ± 2.2	11.8 ± 1.1	17.7 ± 1.6	13.1 ± 1.2	19.0 ± 1.7	14.7 ± 1.3
3DG03	13.2 / 3.6	22.5 / 3.1	8.2 / 5.0	13.9 / 4.9	8.7 / 4.8	16.0 / 3.6	12.3 / 4.3
	16.8 ± 1.5	25.6 ± 2.3	13.2 ± 1.2	18.8 ± 1.7	13.5 ± 1.2	19.6 ± 1.7	16.7 ± 1.5
3DG04	14.8 / 1.0	24.6 / 1.0	9.7 / 2.0	15.5 / 2.3	10.8 / 2.1	17.8 / 1.4	13.5 / 1.3
	15.9 ± 1.4	25.6 ± 2.3	11.8 ± 1.1	17.8 ± 1.6	12.9 ± 1.1	19.2 ± 1.7	14.8 ± 1.3
3DG06	13.5 / 2.7	22.4 / 2.4	8.6 / 4.0	14.1 / 4.0	9.4 / 3.8	16.2 / 2.8	12.1 / 3.3
	16.1 ± 1.4	24.7 ± 2.2	12.5 ± 1.1	18.0 ± 1.6	13.2 ± 1.2	19.0 ± 1.7	15.4 ± 1.4
3DG08	15.2 / 2.0	25.0 / 1.7	10.1 / 3.0	15.8 / 3.3	11.4 / 2.9	18.2 / 2.3	13.8 / 2.2
	17.1 ± 1.5	26.7 ± 2.4	13.0 ± 1.2	19.1 ± 1.7	14.3 ± 1.3	20.4 ± 1.8	15.9 ± 1.4
3DG09	15.0 / 3.6	24.8 / 3.3	9.8 / 5.1	15.6 / 5.0	10.8 / 5.0	17.9 / 3.6	13.5 / 4.6
	18.5 ± 1.7	28.0 ± 2.5	15.0 ± 1.4	20.5 ± 1.8	15.8 ± 1.4	21.6 ± 1.9	18.1 ± 1.6
3DG10	17.0 / 1.2	27.4 / 1.0	11.8 / 2.2	17.7 / 2.5	13.0 / 1.9	20.3 / 1.6	15.5 / 1.3
	18.2 ± 1.6	28.3 ± 2.5	14.0 ± 1.3	20.2 ± 1.8	14.9 ± 1.3	21.9 ± 1.9	16.8 ± 1.5
3DG11	15.4 / 2.6	25.2 / 2.3	10.4 / 3.9	16.1 / 3.9	11.4 / 3.7	18.4 / 2.8	14.0 / 3.2
	18.0 ± 1.6	27.4 ± 2.4	14.2 ± 1.3	20.0 ± 1.8	15.1 ± 1.3	21.2 ± 1.9	17.1 ± 1.5
3DG13	13.2 / 1.3	22.3 / 1.1	8.2 / 2.4	13.8 / 2.6	8.7 / 2.1	15.9 / 1.7	12.2 / 1.5
	14.5 ± 1.3	23.4 ± 2.1	10.5 ± 1.0	16.4 ± 1.5	10.9 ± 1.0	17.6 ± 1.6	13.7 ± 1.2
3DG14	14.7 / 1.0	24.4 / 1.0	9.6 / 2.0	15.3 / 2.3	10.6 / 2.1	17.6 / 1.4	13.4 / 1.3
	15.7 ± 1.4	25.4 ± 2.3	11.6 ± 1.1	17.6 ± 1.6	12.7 ± 1.1	19.0 ± 1.7	14.7 ± 1.3
3DG15	13.4 / 4.0	22.7 / 3.5	8.4 / 5.5	14.1 / 5.4	9.0 / 5.3	16.2 / 4.0	12.5 / 4.9
	17.5 ± 1.6	26.2 ± 2.3	14.0 ± 1.3	19.4 ± 1.7	14.3 ± 1.3	20.2 ± 1.8	17.4 ± 1.5
3DG16	13.2 / 4.1	22.3 / 3.5	8.2 / 5.5	13.8 / 5.4	8.8 / 5.3	15.9 / 4.0	12.2 / 4.9
	17.3 ± 1.5	25.8 ± 2.3	13.8 ± 1.2	19.2 ± 1.7	14.1 ± 1.2	20.0 ± 1.8	17.1 ± 1.5
3DG17	13.4 / 3.2	22.4 / 2.9	8.5 / 4.6	14.0 / 4.6	9.4 / 4.4	16.2 / 3.3	12.1 / 4.0
	16.7 ± 1.5	25.2 ± 2.2	13.1 ± 1.2	18.6 ± 1.7	13.8 ± 1.2	19.5 ± 1.7	16.1 ± 1.4
3DG18	22.7 / 4.1	34.4 / 3.7	18.2 / 5.7	23.2 / 5.5	18.2 / 5.5	26.8 / 4.1	21.2 / 5.1
	26.8 ± 2.4	38.1 ± 3.4	23.9 ± 2.1	28.7 ± 2.5	23.7 ± 2.1	30.9 ± 2.7	26.3 ± 2.3
3DG19	13.3 / 3.9	22.5 / 3.4	8.3 / 5.4	13.9 / 5.2	8.9 / 5.1	16.0 / 3.9	12.3 / 4.7
	17.2 ± 1.5	25.9 ± 2.3	13.7 ± 1.2	19.1 ± 1.7	14.0 ± 1.2	19.9 ± 1.8	17.0 ± 1.5
3DG20	13.4 / 3.4	22.5 / 3.0	8.4 / 4.8	14.0 / 4.8	9.1 / 4.6	16.1 / 3.5	12.3 / 4.2
	16.8 ± 1.5	25.6 ± 2.3	13.3 ± 1.2	18.8 ± 1.7	13.7 ± 1.2	19.6 ± 1.7	16.5 ± 1.5
3DG21	13.4 / 3.9	22.7 / 3.4	8.5 / 5.4	14.1 / 5.3	9.1 / 5.2	16.2 / 3.9	12.5 / 4.8
	17.4 ± 1.6	26.1 ± 2.3	13.8 ± 1.3	19.3 ± 1.7	14.2 ± 1.3	20.1 ± 1.8	17.3 ± 1.5
3DG24	14.6 / 1.0	24.3 / 0.9	9.5 / 2.0	15.2 / 2.3	10.5 / 2.0	17.5 / 1.4	13.3 / 1.2
	15.6 ± 1.4	25.2 ± 2.3	11.5 ± 1.0	17.5 ± 1.6	12.5 ± 1.1	18.9 ± 1.7	14.6 ± 1.3
3DG25	19.5 / 1.9	31.1 / 1.6	14.0 / 2.9	20.2 / 3.2	15.9 / 2.8	23.2 / 2.2	17.5 / 2.0
	21.4 ± 1.9	32.6 ± 2.9	16.9 ± 1.5	23.4 ± 2.1	18.7 ± 1.6	25.4 ± 2.2	19.6 ± 1.7
3DG26	14.0 / 0.9	23.6 / 0.9	8.9 / 1.9	14.6 / 2.2	9.2 / 1.9	16.8 / 1.4	12.9 / 1.1
	14.9 ± 1.3	24.4 ± 2.2	10.7 ± 1.0	16.8 ± 1.5	11.1 ± 1.0	18.2 ± 1.6	14.1 ± 1.3
3DG27	13.6 / 1.2	23.1 / 1.2	8.6 / 2.3	14.3 / 2.6	9.3 / 2.3	16.4 / 1.6	12.7 / 1.6
	14.9 ± 1.3	24.2 ± 2.2	10.9 ± 1.0	16.8 ± 1.5	11.6 ± 1.0	18.1 ± 1.6	14.3 ± 1.3
3DG28	67.1 / 17.7	92.3 / 14.5	59.8 / 19.9	67.6 / 19.2	59.7 / 20.6	78.1 / 15.8	61.9 / 20.4
	84.8 ± 7.4	106.8 ± 9.3	79.7 ± 6.9	86.8 ± 7.5	80.3 ± 6.9	93.9 ± 8.1	82.3 ± 7.1
3DG29	13.6 / 1.8	22.9 / 1.6	8.6 / 2.9	14.2 / 3.1	9.3 / 2.9	16.4 / 2.1	12.6 / 2.2
	15.4 ± 1.4	24.5 ± 2.2	11.4 ± 1.0	17.3 ± 1.5	12.1 ± 1.1	18.5 ± 1.6	14.8 ± 1.3
3DG30	13.5 / 0.9	22.5 / 0.8	8.6 / 1.8	14.1 / 2.2	9.4 / 1.9	16.2 / 1.3	12.2 / 1.1
	14.3 ± 1.3	23.3 ± 2.1	10.4 ± 1.0	16.2 ± 1.4	11.3 ± 1.0	17.5 ± 1.5	13.3 ± 1.2
3DG31	13.4 / 2.0	22.6 / 1.9	8.4 / 3.3	14.0 / 3.4	8.9 / 3.2	16.1 / 2.3	12.5 / 2.6
	15.4 ± 1.4	24.5 ± 2.2	11.6 ± 1.1	17.3 ± 1.5	12.1 ± 1.1	18.4 ± 1.6	15.1 ± 1.3
3DG32	13.8 / 0.9	23.3 / 0.9	8.7 / 1.9	14.4 / 2.2	9.1 / 1.9	16.6 / 1.3	12.8 / 1.2
	14.8 ± 1.3	24.2 ± 2.2	10.6 ± 1.0	16.6 ± 1.5	11.0 ± 1.0	18.0 ± 1.6	14.0 ± 1.3

	PDP08	PDP09	PDP10	PDP11	PDP12	PDP13	PDP14
3DG02	16.6 / 2.3	16.4 / 1.3	12.5 / 3.0	11.0 / 1.7	8.3 / 1.4	10.0 / 2.0	21.0 / 1.4
	18.9 ± 1.7	17.6 ± 1.6	15.5 ± 1.4	12.6 ± 1.1	9.7 ± 0.9	12.0 ± 1.1	22.4 ± 2.0
3DG03	15.0 / 4.6	14.6 / 3.4	11.0 / 5.5	9.0 / 3.4	6.5 / 3.3	8.1 / 3.8	19.5 / 4.1
	19.6 ± 1.8	18.0 ± 1.6	16.5 ± 1.5	12.4 ± 1.1	9.8 ± 0.9	11.9 ± 1.1	23.6 ± 2.1
3DG04	16.8 / 2.2	16.6 / 1.1	12.8 / 2.8	11.0 / 1.6	8.3 / 1.3	10.1 / 1.9	21.8 / 1.2
	19.0 ± 1.7	17.7 ± 1.6	15.6 ± 1.4	12.6 ± 1.1	9.6 ± 0.9	11.9 ± 1.1	23.0 ± 2.0
3DG06	15.3 / 3.7	15.0 / 2.6	11.4 / 4.5	9.5 / 2.7	7.2 / 2.6	8.9 / 3.1	19.5 / 3.1
	19.1 ± 1.7	17.6 ± 1.6	15.9 ± 1.5	12.3 ± 1.1	9.8 ± 0.9	11.9 ± 1.1	22.6 ± 2.0
3DG08	17.2 / 3.0	17.1 / 2.0	13.1 / 3.6	11.6 / 2.2	8.9 / 2.0	10.7 / 2.5	21.9 / 2.0
	20.2 ± 1.8	19.1 ± 1.7	16.7 ± 1.5	13.9 ± 1.3	10.9 ± 1.0	13.2 ± 1.2	23.8 ± 2.1
3DG09	16.9 / 4.7	16.7 / 3.5	12.8 / 5.7	11.0 / 3.5	8.4 / 3.3	10.2 / 3.8	22.0 / 4.4
	21.6 ± 1.9	20.2 ± 1.8	18.6 ± 1.7	14.5 ± 1.3	11.8 ± 1.1	14.0 ± 1.3	26.4 ± 2.3
3DG10	19.1 / 2.3	19.1 / 1.2	14.6 / 2.8	13.3 / 1.6	10.6 / 1.5	12.5 / 2.0	23.5 / 1.2
	21.4 ± 1.9	20.4 ± 1.8	17.4 ± 1.6	14.9 ± 1.3	12.1 ± 1.1	14.5 ± 1.4	24.7 ± 2.2
3DG11	17.4 / 3.6	17.3 / 2.5	13.2 / 4.4	11.6 / 2.7	9.1 / 2.5	10.9 / 3.0	22.0 / 3.0
	21.1 ± 1.9	19.8 ± 1.8	17.6 ± 1.6	14.3 ± 1.3	11.6 ± 1.1	13.9 ± 1.3	25.0 ± 2.2
3DG13	15.0 / 2.4	14.6 / 1.4	11.0 / 2.9	9.0 / 1.7	6.5 / 1.6	8.2 / 2.1	19.5 / 1.5
	17.4 ± 1.6	15.9 ± 1.4	14.0 ± 1.3	10.7 ± 1.0	8.1 ± 0.7	10.2 ± 1.0	21.0 ± 1.9
3DG14	16.6 / 2.2	16.4 / 1.1	12.6 / 2.8	10.8 / 1.5	8.1 / 1.3	9.9 / 1.8	21.6 / 1.2
	18.8 ± 1.7	17.5 ± 1.6	15.4 ± 1.4	12.3 ± 1.1	9.5 ± 0.9	11.7 ± 1.1	22.7 ± 2.0
3DG15	15.3 / 5.0	14.9 / 3.9	11.3 / 6.0	9.3 / 3.8	6.8 / 3.7	8.4 / 4.1	19.8 / 4.6
	20.3 ± 1.8	18.7 ± 1.7	17.3 ± 1.6	13.1 ± 1.2	10.5 ± 0.9	12.6 ± 1.2	24.4 ± 2.2
3DG16	15.0 / 5.1	14.6 / 3.9	11.0 / 6.0	9.0 / 3.8	6.5 / 3.7	8.2 / 4.1	19.4 / 4.7
	20.0 ± 1.8	18.5 ± 1.6	17.0 ± 1.6	12.8 ± 1.2	10.3 ± 0.9	12.3 ± 1.2	24.1 ± 2.1
3DG17	15.3 / 4.3	15.0 / 3.1	11.4 / 5.1	9.5 / 3.2	7.1 / 3.0	8.8 / 3.5	19.5 / 3.7
	19.6 ± 1.7	18.1 ± 1.6	16.5 ± 1.5	12.7 ± 1.1	10.2 ± 0.9	12.3 ± 1.2	23.2 ± 2.1
3DG18	25.3 / 5.2	25.2 / 4.0	20.3 / 6.3	19.5 / 4.0	17.9 / 3.8	20.0 / 4.3	31.5 / 4.8
	30.6 ± 2.7	29.3 ± 2.6	26.6 ± 2.4	23.5 ± 2.1	21.8 ± 1.9	24.2 ± 2.2	36.3 ± 3.2
3DG19	15.1 / 4.9	14.7 / 3.7	11.1 / 5.8	9.1 / 3.7	6.6 / 3.6	8.3 / 4.0	19.5 / 4.5
	20.0 ± 1.8	18.4 ± 1.6	17.0 ± 1.6	12.8 ± 1.2	10.2 ± 0.9	12.3 ± 1.2	24.0 ± 2.1
3DG20	15.2 / 4.5	14.8 / 3.3	11.3 / 5.3	9.3 / 3.3	6.8 / 3.2	8.5 / 3.7	19.7 / 4.0
	19.7 ± 1.8	18.2 ± 1.6	16.6 ± 1.5	12.6 ± 1.1	10.0 ± 0.9	12.1 ± 1.1	23.6 ± 2.1
3DG21	15.3 / 4.9	14.9 / 3.8	11.3 / 5.8	9.3 / 3.7	6.8 / 3.6	8.4 / 4.0	19.8 / 4.5
	20.2 ± 1.8	18.7 ± 1.7	17.2 ± 1.6	13.0 ± 1.2	10.4 ± 0.9	12.5 ± 1.2	24.3 ± 2.2
3DG24	16.5 / 2.1	16.3 / 1.1	12.5 / 2.7	10.7 / 1.5	8.0 / 1.3	9.8 / 1.8	21.4 / 1.1
	18.7 ± 1.7	17.4 ± 1.5	15.2 ± 1.4	12.2 ± 1.1	9.3 ± 0.9	11.6 ± 1.1	22.6 ± 2.0
3DG25	22.0 / 2.9	22.2 / 1.9	17.5 / 3.5	16.6 / 2.3	13.4 / 2.1	15.7 / 2.6	27.0 / 1.8
	24.9 ± 2.2	24.1 ± 2.1	21.0 ± 1.9	18.9 ± 1.7	15.5 ± 1.4	18.2 ± 1.7	28.8 ± 2.5
3DG26	15.7 / 2.1	15.4 / 1.0	11.6 / 2.5	9.5 / 1.4	7.0 / 1.2	8.7 / 1.7	20.6 / 1.0
	17.8 ± 1.6	16.4 ± 1.5	14.2 ± 1.3	11.0 ± 1.0	8.3 ± 0.8	10.4 ± 1.0	21.6 ± 1.9
3DG27	15.5 / 2.4	15.1 / 1.3	11.5 / 3.1	9.5 / 1.7	6.9 / 1.5	8.5 / 2.0	20.1 / 1.5
	17.9 ± 1.6	16.4 ± 1.5	14.6 ± 1.4	11.2 ± 1.0	8.4 ± 0.8	10.6 ± 1.0	21.6 ± 1.9
3DG28	72.9 / 18.0	75.0 / 16.3	62.6 / 21.0	69.7 / 16.3	67.9 / 15.6	72.6 / 15.7	81.3 / 17.4
	90.9 ± 7.9	91.3 ± 7.9	83.7 ± 7.4	86.0 ± 7.5	83.5 ± 7.3	88.2 ± 7.9	98.7 ± 8.5
3DG29	15.4 / 2.9	15.1 / 1.8	11.4 / 3.5	9.5 / 2.1	6.9 / 1.9	8.6 / 2.4	19.9 / 2.0
	18.3 ± 1.6	16.9 ± 1.5	14.9 ± 1.4	11.5 ± 1.0	8.8 ± 0.8	10.9 ± 1.0	21.9 ± 1.9
3DG30	15.4 / 2.0	15.0 / 1.0	11.4 / 2.5	9.6 / 1.4	7.1 / 1.2	8.8 / 1.7	19.6 / 1.0
	17.4 ± 1.6	16.0 ± 1.4	14.0 ± 1.3	11.0 ± 1.0	8.3 ± 0.8	10.5 ± 1.0	20.6 ± 1.8
3DG31	15.2 / 3.2	14.8 / 2.1	11.2 / 4.0	9.2 / 2.3	6.6 / 2.1	8.3 / 2.6	19.7 / 2.5
	18.3 ± 1.6	16.8 ± 1.5	15.2 ± 1.4	11.4 ± 1.0	8.7 ± 0.8	10.9 ± 1.0	22.2 ± 2.0
3DG32	15.5 / 2.1	15.2 / 1.0	11.5 / 2.6	9.4 / 1.4	6.9 / 1.2	8.5 / 1.7	20.3 / 1.0
	17.6 ± 1.6	16.2 ± 1.4	14.0 ± 1.3	10.8 ± 1.0	8.1 ± 0.7	10.2 ± 1.0	21.3 ± 1.9

Andrew J. Woods is a research engineer with the Centre for Marine Science and Technology at Curtin University of Technology, Perth, Australia. He received his MEng and BEng (Hons1) degrees in electronics engineering and has nearly 20 years experience in the design, application, and evaluation of stereoscopic imaging solutions for teleoperation, industrial, and entertainment applications. He is co-chair of the annual Stereoscopic Displays and Applications Conference (since 2000) and in 2005 was co-chair of the annual Electronic Imaging: Science & Technology Symposium.

Ka Lun Yuen is a graduate of Curtin University of Technology with a double bachelors degree in physics and education.

Kai S. Karvinen is currently completing a double bachelors degree in physics and electrical engineering at Curtin University of Technology and is a tutor in the Department of Electrical Engineering at Curtin University of Technology.